The following publication M. Ghafouri, U. Karaagac, J. Mahseredjian and H. Karimi, "SSCI Damping Controller Design for Series-Compensated DFIG-Based Wind Parks Considering Implementation Challenges," in IEEE Transactions on Power Systems, vol. 34, no. 4, pp. 2644-2653, July 2019 is available at https://dx.doi.org/10.1109/TPWRS.2019.2891269.

SSCI Damping Controller Design for Series Compensated DFIG based Wind Parks Considering Implementation Challenges

Mohsen Ghafouri, *Student Member, IEEE*, Ulas Karaagac, *Member*, *IEEE,*
Jean Mahseredjian, *Fellow, IEEE*, Houshang Karimi, *Senior Member*, *IEEE*

***Abstract*— The use of supplementary controllers for mitigating subsynchronous control interaction (SSCI) in DFIG-based wind parks is quite promising due to their low investment costs. These SSCI damping controllers are typically designed and tested using an aggregated wind turbine (WT) model that represents the entire wind park (WP). However, no research has been reported on their implementations in a realistic WP. This paper first presents various implementation schemes for a linear-quadratic regulator (LQR)-based SSCI damping controller, and discusses the corresponding practical challenges. Then, an implementation scheme which obviates the need for high rate data transfer between the WTs and the WP secondary control layer is proposed. In the proposed implementation, the SSCI damping controller receives only the WT outage information updates from the WP controller (WPC), hence it is not vulnerable to the variable communication network latency. The SSCI damping controller parameters are also modified when there is a change in WT outage information for the ultimate performance. The effectiveness of the proposed implementation scheme is confirmed with detailed electromagnetic transient (EMT) simulations, considering different wind speed at each WT and WT outages due to sudden decrease in wind speeds.**

***Index Terms*— Detailed design, doubly-fed induction generator (DFIG), optimal control, series capacitor compensation, subsynchronous control interaction (SSCI), wind park.**

I. Introduction

Subsynchronous control interaction (SSCI) is the interaction between the power electronics control and the series compensated transmission system that occurs at frequencies below the system synchronous frequency. The SSCI may occur between a doubly-fed induction generator (DFIG) driven by wind turbine (WT), and the series compensated transmission line [1]. This phenomenon has been observed in US and China [2]-[5]. There has been recently a growing interest in developing effective SSCI mitigation methods [6].

Countermeasures against SSCI, includes detection algorithms to trip the WTs [2],[7]; bypass filters across the series capacitor [8]; phase imbalanced series capacitive compensation [9]; and approaches using flexible ac transmission systems (FACTS) (for example, static var compensator (SVC) [10],[11]; static synchronous compensator (STATCOM) [12]; thyristor controlled series capacitor (TSC) [13]; and gate controller series capacitor (GCSC) [13]-[16]).

The mitigation methods based on the application of supplementary control signal (or signals) in DFIG converter control part of the WT control (WTC) [9], [17]-[23] are quite promising due to their low investment costs. The supplementary SSCI damping controller has been designed based on static state feedback control [17]-[19], partial feedback linearization (PFL) [20], adaptive control [21], two degree of freedom (2DOF) controller [22], lead-lag controller [9], and proportional-integral (PI) regulator [23]. On the other hand, further research is required to conclude on the effectiveness and/or feasibility of those proposed methods as none of them discuss implementation challenges in a realistic WP. Only [17] considers a WP with a realistic reactive power control scheme and designs the SSCI damping controller considering the potential negative impact on the WT transient response during faults.

Among the design approaches, static state feedback control scheme is an effective and simple one [17]-[19]. The linear-quadratic regulator (LQR) technique is one of the well-established controller design techniques based on the state feedback theory. The use of this technique results in an optimal and robust controller, which ensures at least 60 degrees phase margin, while preserving the order of the closed-loop system similar to the plant. Moreover, this technique enables to adjust the controller parameters to achieve the effective usage of the available converter capacity. The LQR technique also does not change the order of the closed loop system, hence it results in a lower degree closed-loop system compared to many other techniques used in literature.

In such control structure, the states of the overall system are first estimated by an observer, and then utilized to damp the oscillation using a supplementary controller. Despite their satisfactory performance, these controllers require the mathematical model of the system which may change depending on the system operating conditions. They are also

M. Ghafouri, J. Mahseredjian and H. Karimi are with Polytechnique Montreal, Montreal (Quebec), Canada;

U. Karaagac is with The Hong Kong Polytechnic University, Hong Kong, China.

designed to operate in the secondary control layer of the WP as the entire system inside the WP is represented with a single aggregated WT. In such control scheme, the DFIG converter currents of each WT are measured and transmitted to a central SSCI damping controller as input signals. The output signals of the central SSCI damping controller are also sent back to the WTCs as input signals. This control scheme may be subjected to noise, sensor delay or failure, and requires communication links between the WTs and the central SSCI damping controller with high transfer rate of data. An alternative approach is integrating the SSCI damping controller into the WTC (if possible). This scheme is referred to as local SSCI damping controller as the damping controller uses only the local measurements.

This paper proposes a local SSCI damping controller with outputs injected into the inner control loops of the DFIG converters. The proposed controller is designed based on the linear-quadratic regulator (LQR) technique [17] using the simple linearized system model. The proper function of the local SSCI damping controller is achieved by scaling the DFIG converter currents considering WT outages in the WP. This information is available at the WP controller (WPC) and changes whenever there is a change in the number of WTs in service (i.e. no continuous change). Hence, the high rate data transfer between the WTs and the secondary control layer of the WP is not required. Further performance improvement in achieved by modifying the controller parameters considering the WT outages. This adaptive scheme is achieved by designing several controllers for different number of WTs in service. The permissible slowest wind speed is considered in SSCI damping controller design where the system is most vulnerable to SSCI.

The effectiveness of the proposed local LQR-based adaptive SSCI damping controller and its superiority over its traditional version (i.e. LQR-based central SSCI damping controller) is confirmed with detailed electromagnetic transient (EMT) simulations. The EMT model of DFIG [24] used in this paper includes all the nonlinearities (in both electrical and control system model) and essential transient functions to fulfill the grid code requirement regarding FRT [25]. In EMT simulations, the WP includes the detailed medium voltage (MV) collector grid model and different wind speeds are applied to each WT considering a reasonable Gaussian distribution. Representative simulations with aggregated model are also performed to confirm the accuracy of the aggregated model that uses the average wind speed.

The major contributions of the paper are summarized below:

- A local SSCI damping control implementation scheme that eliminates the high rate data transfer requirement between the WTs and secondary control layer of the WP as well as makes the communication system immune to the excessive (even unrealistic) communication delays;
- An improved LQR-based SSCI damping controller performance through an adaptive approach;
- Accuracy validation for the average wind speed assumption based aggregated wind park model which is traditionally used during SSCI damping controller design as well as in the system wide studies.

It should be emphasized that, the existing researches in the literature disregard the physical structure of the WPs by considering the entire WP as a single large WT. Hence the potential implementation difficulties and problems of the proposed SSCI damping controllers never discussed. This paper presents the first detailed discussion on the implementation of SSCI damping control in practical WPs.

The paper is organized as follows. The description of the WP and its control structure are presented in Section II. Section III briefly describes the design procedure of the controller. The proposed implementation scheme is addressed in Section IV. The EMT simulations of the test system are presented in Section V.

II. Wind Park with DFIG Wind Turbines

As shown in Fig. 1, the power produced by the WTs are transmitted to the point of interconnection (POI) through the MV collector grid and WP transformer. Usually, the WP transformer has an on-load-tap-changer (not shown in Fig. 1) to keep the MV collector bus voltage around its nominal value.

The active power at POI (see Fig. 1) depends on the wind conditions at each WTG inside the WP and determined by maximum power point tracking (MPPT) function. On the other hand, the WP reactive power control is based on the secondary voltage control concept [24],[26]. At the primary level, the WTC monitors and controls its own positive sequence terminal voltage (V_{dfig}) with a proportional voltage regulator. At the secondary level, the WPC modifies the WTC reference voltage values (V'_{dfig}) via a proportional-integral (PI) reactive power regulator to achieve the desired reactive power flow at POI when operating under reactive power control function. A typical WPC also includes voltage and power factor control functions. Reader should refer to [24] for details. This paper considers WPC operating under reactive power control function.

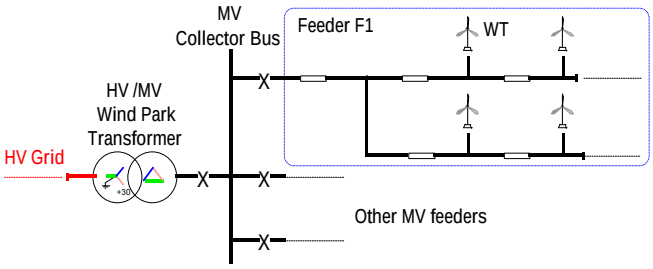

Fig. 1. A simplified single-line diagram of a typical wind park.

In DFIG WTs, the stator of the induction generator (IG) is directly connected to the grid. The wound rotor of the IG is connected to the grid through an ac-dc-ac converter system consists of two three-phase pulse-width modulated converters (Rotor-Side Converter (RSC) and Grid-Side Converter (GSC)). A line inductor and shunt harmonic ac filters are utilized at the GSC for improving the power quality. A crowbar is used for RSC overcurrent and dc capacitor overvoltage protection. The RSC is blocked and the IG consumes reactive power during

crowbar operation. To avoid its operation during faults, a dc resistive chopper is widely used to limit the dc voltage.

The considered control scheme is illustrated in Fig. 2. The RSC operates in the stator flux reference frame and the GSC operates in the stator voltage reference frame. q- and d-axis currents of the RSC (i_{qr} and i_{dr}) are used to control the active power output and positive sequence terminal voltage of the DFIG (P_{dfig} , V_{dfig}), respectively. d-axis current of GSC (i_{dg}) is used to regulate the dc bus voltage (V_{dc}) and q-axis current of GSC (i_{qg}) is used to support the grid with reactive power during faults. In Fig. 2 and henceforward, all variables are in pu and primed variables are used to indicate the reference values transmitted from controllers.

Both RSC and GSC are controlled by a two-level controller. The slow outer control calculates the reference dq-frame currents and the fast inner control allows controlling the converter ac voltage reference. The reference for DFIG active power output (P'_{dfig}) is given by the MPPT algorithm. The reference for DFIG positive sequence voltage (V'_{dfig}) is modified by the WPC. $\Delta V'_{dfig}$ in Fig. 2 is the output of the WPC PI reactive power regulator.

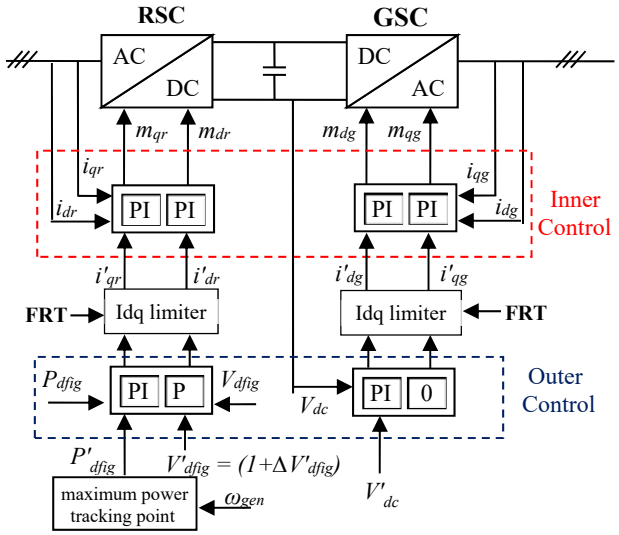

Fig. 2. Schematic diagram of the DFIG wind turbine control.

During normal operation, GSC operates at unity power factor ($i'_{dg} = 0$) and RSC controller gives the priority to the active current.

The grid code requirements, such as [25], include the WT transient response against severe voltage disturbances. To comply with this requirement, an FRT function is traditionally added to the WTC. The FRT function becomes active following a severe voltage sag or swell condition, and it modifies the active and reactive current references produced by the outer loop of the WTC considering the grid code requirement. This paper considers a DFIG WT that has an FRT function compliant with the requirement in [25]. Reader should refer to [24] for details.

III. SSCI Damping Controller

The radially compensated wind park model used in the SSCI damping controller design is shown in Fig. 3. The model disregards all shunt branches except the DFIG aggregated harmonic filters. The series RLC branch in Fig. 3 represents the aggregated DFIG transformers, the equivalent collector grid, the aggregated WP transformers and the series compensated high voltage (HV) grid.

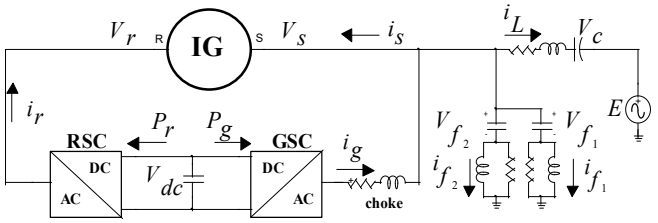

Fig. 3. Radially compensated wind park model used in SSCI damping controller design.

The linearized state-space representation of the system can be described as follows:

$$\begin{aligned} \dot{\mathbf{x}} &= \mathbf{A}\mathbf{x} + \mathbf{B}\mathbf{u} \\ \mathbf{y} &= \mathbf{C}\mathbf{x} + \mathbf{D}\mathbf{u} \end{aligned} \tag{1}$$

where $\mathbf{x}$, $\mathbf{u}$ and $\mathbf{y}$ denote the vectors of the system states, inputs, and outputs, respectively. The matrices $\mathbf{A}$, $\mathbf{B}$, $\mathbf{C}$ and $\mathbf{D}$ determines the small signal behavior of the linear system.

The LQR control scheme consists of a full-state observer and a static gain controller [27]. The design procedure in [17] is adopted in this paper. The RSC and GSC currents in dq reference frame ($[i_{qr}\ i_{dr}\ i_{qg}\ i_{dg}]^T$) are selected as the inputs of the controller. The outputs of the controller ($[u_{qr}\ u_{dr}\ u_{qg}\ u_{dg}]^T$) are augmented into the current control loops of the DFIGs. The LQR controller is designed using the linearized model of the system, and $\mathbf{Q}$ and $\mathbf{R}$ matrices. These matrices denote the coefficients of state and control signals in a trade-off between the energies of the control signals and the controlled outputs. The LQR controller is then obtained by solving the Ricatti equations. In this paper, $\mathbf{Q}$ is assumed to be equal to $\mathbf{C}^T\mathbf{C}$ and $\mathbf{R}$ is adjusted by considering the system response following large disturbances such as faults. This step requires performing several EMT simulations and updating the matrix $\mathbf{R}$ accordingly. The matrix $\mathbf{R}$ should be selected to use the maximum available capacity of the DFIG converters for SSCI damping. It should be noted that large control effort will cause converter saturation. Initially, the matrix $\mathbf{R}$ is set to be unity matrix with appropriate dimension (i.e. $\mathbf{R} = \mathbf{I}$), and updated based on EMT simulation results to achieve an acceptable converter capacity usage. The behavior during severe voltage sags (due to fault) is disregarded as the output signals of the controller are limited dynamically to ensure the desired DFIG response during normal and FRT operations [17].

The main aim of the observer is to estimate the state vector of the system ($\hat{\mathbf{x}}$). To stabilize the internal dynamics of the observer error ($\mathbf{e} = \mathbf{x} - \hat{\mathbf{x}}$), the gain of the observer ($\mathbf{L}$) is obtained using the linear matrix inequality (LMI) technique. The observer design is the pole placement of $\mathbf{A} - \mathbf{LC}$

eigenvalues. This technique enables the designer to adjust the fastness of the error dynamic ($\mathbf{A}-\mathbf{LC}$) by moving its eigenvalues far to the left half plane. However, a very fast observer will result in a control system which is sensitive to measurement noise. The corresponding observer gain matrix ($\mathbf{L}$) is designed based on the method discussed in [28] as:

$$\mathbf{L}=(\mathbf{W}\,\mathbf{P}_{\mathbf{LMI}}^{-1})^{T} \tag{2}$$

where

$$\mathbf{A}^{T}\mathbf{P}_{\mathbf{LMI}}+\mathbf{A}\,\mathbf{P}_{\mathbf{LMI}}-\mathbf{C}^{T}\mathbf{W}-\mathbf{W}^{T}\mathbf{C}+2\gamma\,\mathbf{P}_{\mathbf{LMI}}<\mathbf{0} \tag{3}$$

$\mathbf{P}_{\mathbf{LMI}}>\mathbf{0}$ and $\mathbf{W}$ are the solutions of the LMI described in (3), and γ is a parameter corresponded to the fastness of the observer.

The observer is designed to shift the poles of the closed-loop system into a region with real value less than -10 (i.e. $\mathrm{Re}(s)<-10$). These values are obtained through EMT simulations of the considered system and provide the desired transient response. The details can be found in [17], [27].

IV. Proposed Implementation

The SSCI damping controller is designed based on the aggregated WT model. As the entire WP is represented with a single WT during design (although the WPC is taken into account), the designed controller requires the sum of RSC and GSC currents of the WTs. Hence, it is expected to be located in the secondary control layer of the WP. In this implementation, each WTC sends the DFIG converter current measurements to the central SSCI damping controller (α in Fig. 4) and receives the output signal of the central SSCI damping controller (β in Fig. 4). This implementation requires communication links that enables high rate data transfer between the WTs and the central SSCI damping controller.

Fig. 5 shows the proposed local SSCI damping controller in which it is integrated into the DFIG control. This implementation will not function properly when there are significant WT outages in the WP. On the other hand, the wind conditions and reactive power generation at each WT is expected to be similar. Hence, proper function of SSCI damping controller can be achieved by scaling the measured DFIG converter currents considering the number of units in service (N in Fig. 5). It should be emphasized here that, the aggregated model used for SSCI damping controller design also assumes the same wind conditions and reactive power generation at each WT. The status of WTs as well as the status of WT certain protection relays are transmitted to the WPC through a low-speed communication link between WPC and WTs. Hence, the information N is available at WPC and can be transmitted to WTCs with the voltage reference generated by the WPC ($\Delta V'_{dfig}$ in Fig. 2). The signal N only changes whenever there is a change in the number of WTs in service (i.e. no continuous change). Hence, the high rate data transfer between the WTCs and the WPC is not required. It should be noted that, sudden and large changes in N can be expected following a fault inside the WP or following a sudden drop in the wind speed that results into partial tripping in the WP due to different wind conditions at each WT.

In order to improve the SSCI damping controller performance, this paper proposes an adaptive approach that modifies the controller considering number of units in service. In this approach, a separate SSCI damping controller (i.e. LQR gain and observer) is designed for each WT outage scenario, and the selection is made with the signal N (i.e. the number of WTs in service) as illustrated in Fig. 6.

The adaptive approach used in this paper switches the SSCI damping controller based on the gain scheduling technique. 10 different controllers are designed for 10 different WT outage scenarios from zero to 90%. For example when 50 WTs are out of service in a 268 WT wind park, (i.e. N = 218), the controller switches to the parameters designed for 20% (50/268 = 18.7%) WT outage scenario. The performance of this adaptive approach can be improved further considering the wind speed in addition to the WT outage scenarios. On the other hand, the improvement is quite marginal and the corresponding results are not presented in the paper.

It should be noted that, the same adaptive approach can be also used in the central SSCI damping controller (see Fig. 4) as the number of WTs in service is known at secondary control level.

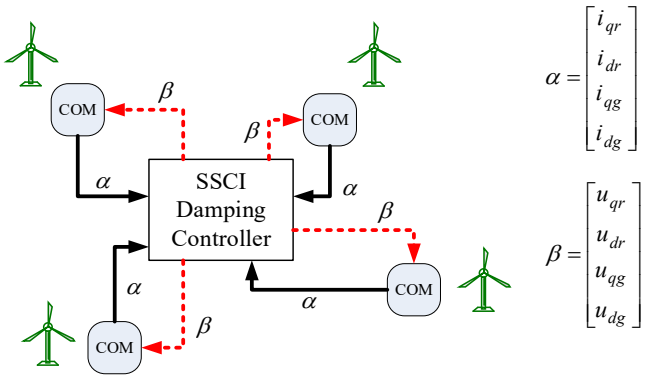

Fig. 4. Central implementation scheme of the SSCI damping controller.

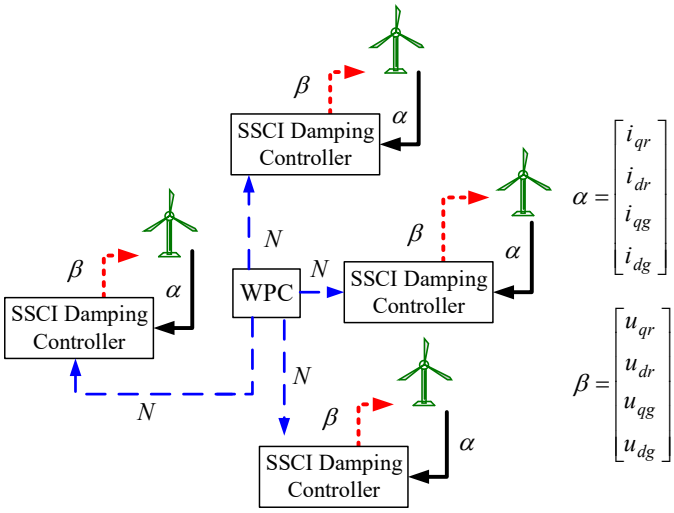

Fig. 5. Proposed local implementation scheme of the SSCI damping controller.

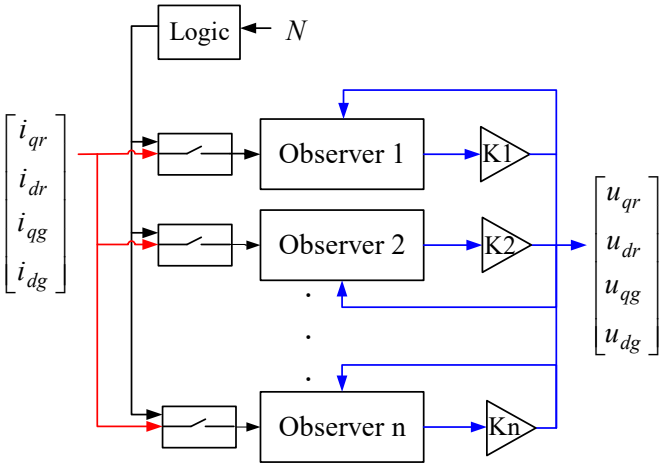

Fig. 6. Local SSCI damping controller schematic.

V. Study System

To assess the proposed SSCI damping controller performance, the 500 kV system shown in Fig. 7 is adopted as test system. The WP consists of 1.5 MW 268 DFIG WTs and connected to two large systems, System-1 and System-2, through the transmission lines Line-1 and Line-2. Line-1 is series compensated with 50% compensation level using two identical capacitor banks located at its ends. When Line-2 is disconnected, it leaves the wind park radially connected to the series capacitor compensated line Line-1. The circuit breakers CB1 and CB2 are used to clear the faults on Line-2. Reader should refer to [17] for the details of the 500 kV system and the impact of wind park operating conditions (wind speed, reactive power generation, WT outage) on SSCI mode damping.

The SSCI damping controller is designed using the average wind speed assumption based aggregated model of WP for the operating condition in which the SSCI problem is most severe (i.e. the permissible slowest wind speed and 132 WT in service). The effectiveness of the controller has been already validated in [17] through EMT simulations for various operating conditions using the aggregated model of the WP.

The focus of this paper are to discuss the SSCI damping control implementation challenges in a realistic WP and to propose practicable and effective implementation methods. Hence, detailed EMT model of the WP is considered. As shown in Fig. 8, the considered wind park is divided into four clusters and connected to the 500 kV power system through two wind park transformers (WF TR-1 and WF TR-2). Each cluster is assumed to be same and contains 67 WT on five 34.5 kV feeders. The WP cluster is inspired from an actual system and one of the feeders is presented in Fig. 9.

VI. EMT Simulations

The EMT simulations are performed using EMTP [29] using the generic models in [24] for the WTs. The DFIG converters are represented with average value models (AVMs). The simulation time step is 50 μs.

A three-phase metallic fault is applied at wind park end of Line-2 at t = 1.2 s and cleared with the operation of circuit breakers CB1 and CB2 (as shown in Fig. 7). The operating times of CB1 and CB2 are 80 and 60 ms, respectively. The simulation scenarios are presented in Table I. σ(η,β) represents the Gaussian distribution with mean value and standard deviation of η and β, respectively. It should be noted that, SSCI problem is more severe at slow wind speeds. At 0.8 pu wind speed and higher, the SSCI damping controller exhibits much better performance, hence not presented here.

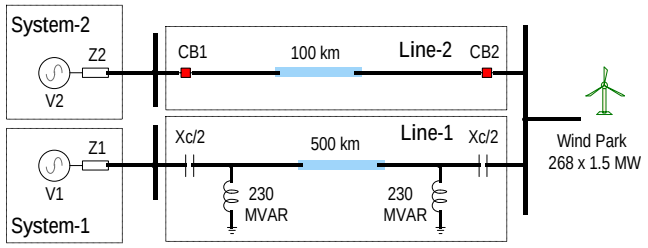

Fig. 7. The case study system

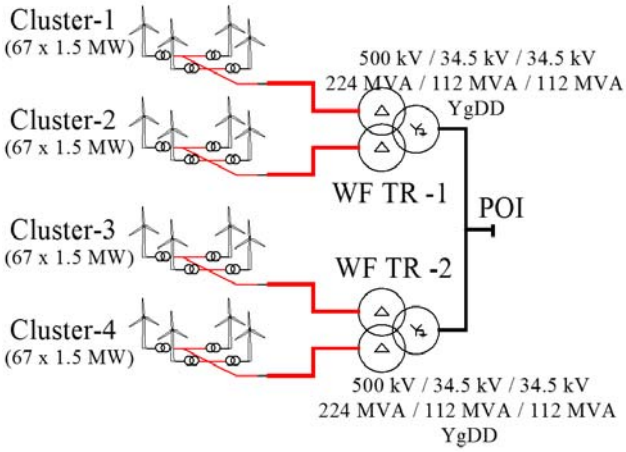

Fig. 8. Simplified single line diagram of the wind park.

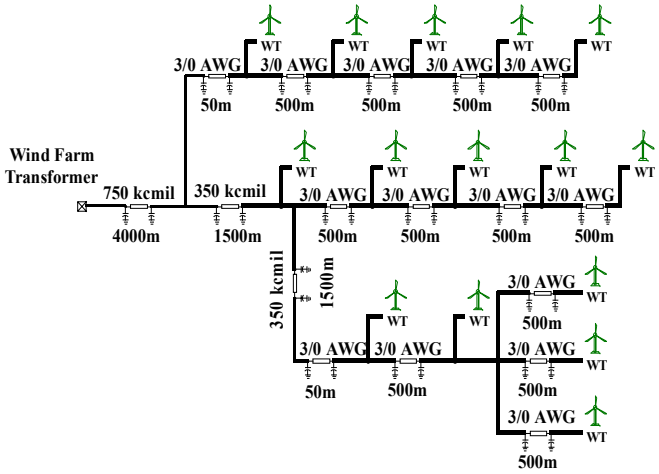

Fig. 9. The detailed model of the feeder with 15 DFIGs.

Table I: Simulation Scenarios

Scenario	SSCI Controller	Wind Speed	Outage
S1	No SSCI controller	σ (0.7pu,0.1pu)	No outage
S2	Central SSCI controller	σ (0.7pu,0.1pu)	No outage
S3	Central SSCI controller with 2 ms delay in feedback loop	σ (0.7pu,0.1pu)	No outage
S4	Local SSCI controller	σ (0.7pu,0.1pu)	No outage
S5	Central SSCI controller	σ (0.7pu,0.1pu)	34 x 4 WTs
S6	Local SSCI controller	σ (0.7pu,0.1pu)	34 x 4 WTs
S7	Central SSCI controller	0.6 pu	No outage
S8	Local SSCI controller	0.6 pu	No outage
S9	Local SSCI controller	0.6 pu	34 x 4 WTs
S10	Local SSCI controller	0.6 pu	Cluster I and II
S11	Local SSCI controller	0.6 pu	Sudden outage of 34x4 WTs at 1.5s
S12	Local SSCI controller with 20 ms delay in feedback loop	0.6 pu	Sudden outage of 34x4 WTs at 1.5s

The WT outages in simulation scenarios S5, S6, S9 and S10 (see Table I) are assumed to take place prior the fault simulation. For example, there are 132 WTs in service inside the WP in steady-state. On the other hand, in the simulation scenarios S11 and S12, there are 268 WTs in service (i.e. no WT outages) and outage of 136 WTs takes place suddenly at the 1.5s of the simulation. These sudden WT outage scenarios (i.e. S11 and S12) are essential to demonstrate the immunity of the proposed local SSCI damping controller implementation to the excessive (even unrealistic) communication delays. Moreover, these simulations will also confirm the effectiveness of the proposed gain scheduling scheme following a large amount of sudden WT outage just after the fault (i.e. before the SSCI oscillations damped completely).

The effectiveness of the proposed controllers is shown in Fig. 10. The system becomes unstable in S1 following to fault removal. On the other hand, the system becomes stable with the proposed local and central SSCI damping controllers. Although all units are in service in scenarios S1 - S4 (i.e. the adaptive approach implemented at the local SSCI controller has no impact), the local SSCI controller exhibits better performance in S4 compared to its central implementation counterpart in S2. The reason is the different wind speed conditions and different reactive power generations at each WT. It should be noted that, the central SSCI damping controller uses the total active and reactive currents produced by the WT converters. This results an averaging effect. Moreover, all WTCs receive the same signal from the central SSCI damping controller although their operating conditions are different. On the other hand, each local SSCI damping controller produces its output signal based on the WT operating condition.

The delay sensitivity of central implementation is illustrated in Fig. 11. The system does not remain stable when there is 2 ms delay in the feedback loop.

The unstable operation in simulation scenario S3 can be also identified using frequency scan based analysis. In this method, the impedance characteristics of the turbine for the subsynchronous range is obtained through EMT type simulations [30], [31], [32]. On the other hand, the grid side impedance is obtained with traditional frequency scanning technique. The SSCI prediction is made by adding the turbine side and grid side impedances [30] (combined scan analysis). Any reactance crossover in combined scan with negative total resistance indicates potential SSCI. The details of the utilized frequency scanning method can be found in [30].

In this study, the turbine side frequency scanning is performed using the aggregated model for 132 WTs and 0.6 pu wind speed. The 2 ms delay is applied in the feedback loop of the aggregated model to obtain the impedance characteristics of the turbine for the simulation scenario S3. The combined scan analysis (the sum of turbine side and grid side impedances) are presented in Fig. 12. Unlike scenario S2, the total resistance (R) is negative in simulation scenario S3 at the reactance crossover frequency.

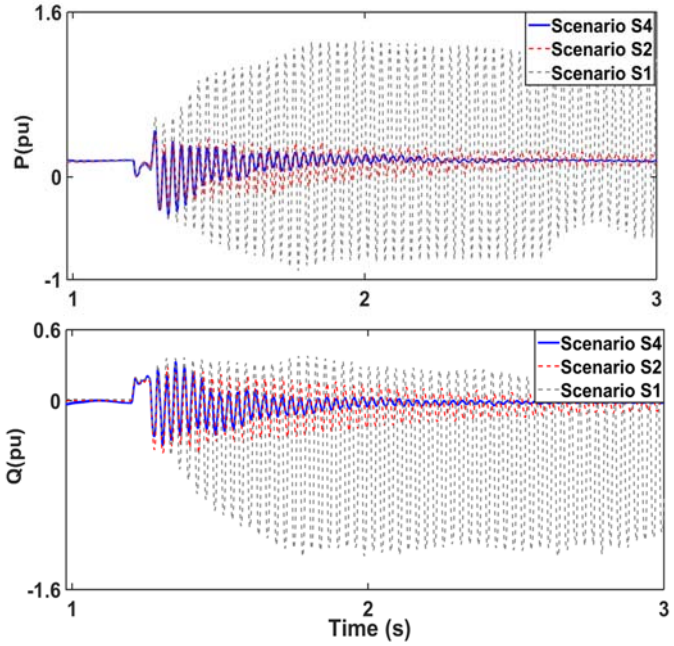

Fig. 10. Active and reactive powers in scenarios S1, S2 and S4.

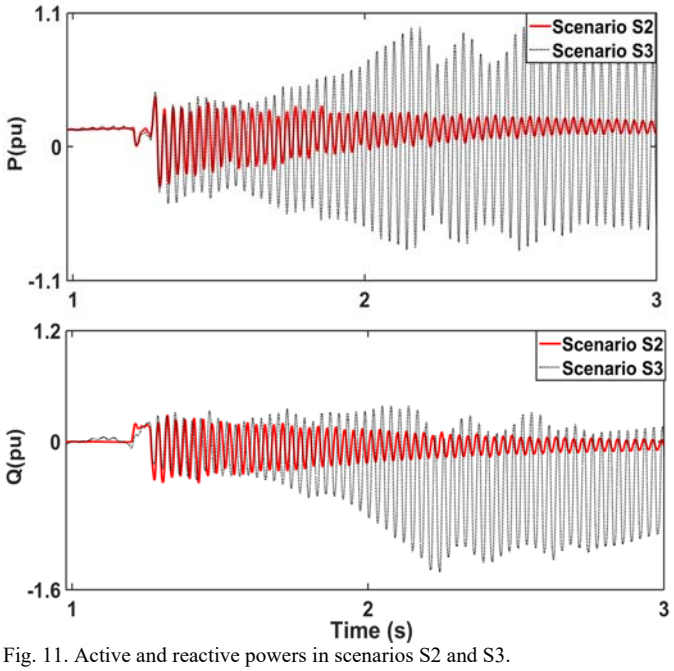

Fig. 11. Active and reactive powers in scenarios S2 and S3.

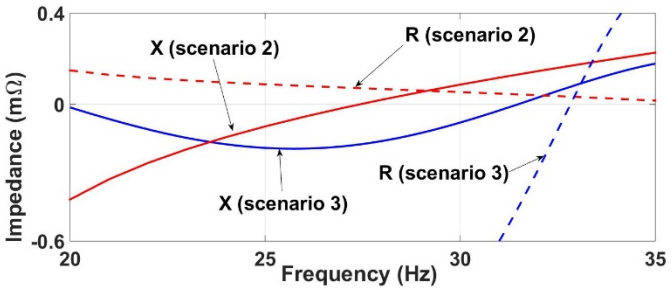

Fig. 12. Combined scans for simulation scenarios S2 and S3.

The impact of implemented adaptive approach on SSCI damping controller becomes apparent in Fig. 13 which presents the 136 WT outage simulation scenarios for σ (0.7pu, 0.1pu) wind speed. The SSCI damping controller in S6 modifies controller parameters considering the number of units in service, and achieves much better performance compared to its central implementation counterpart in S5. It should be noted that, the performance difference between central and local SSCI damping controllers become less noticeable when the parameters of the central control are also modified for the number of WTs in service.

The effectiveness of both controllers can be seen in Fig. 14 for the permissible slowest wind speed (0.6 pu). In this scenario, there is no WT outage and the wind speeds are same at all WTs. Hence, the performance difference between the local and central SSCI damping controllers only results from the different reactive power generation at each WT. As seen from Fig. 14, the performance difference is not significant compared to the simulation scenarios in Fig. 10, and Fig. 13.

The results presented in Fig. 15 confirm the effectiveness of the proposed local SSCI controller at the permissible slowest wind speed for various extreme WT outage scenarios. Modifying the SSCI controller parameters for the WT outages provides the ultimate performance. Moreover, as shown in Fig. 16, the proposed implementation does not only eliminate the high rate data transfer requirement between the WTs and the secondary control layer of the WP, but also make the system immune to the excessive (even unrealistic) communication delays. As illustrated in Fig. 11, the central implementation counterpart is very vulnerable to communication delays and its usage may not be feasible in practice.

This paper considers fixed series capacitor compensation. However, the effective compensation level may decrease during operation due to outages in the system (i.e. increase in the equivalent reactance). Moreover, one of the series capacitors can be bypassed by the overvoltage protection during fault and it may not be reinserted immediately after the fault clearance if spark gaps are used for overvoltage protection. It should be noted that the system is less vulnerable when the series compensation level decreases. To demonstrate the effectiveness of the proposed controller, the remote series capacitor is bypassed following the fault in the simulation scenario S9. The results are presented in Fig. 17 and confirm the effectiveness of the proposed controller.

The effective compensation level may increase due to investments in the system (such as new transmission lines and power plants), i.e. due to decrease in the equivalent impedance of System-1 in the simulation model. To demonstrate the effectiveness of the proposed controller, the equivalent impedance of System-1 is reduced to 75% in the simulation scenario S9. The compensation level should be increased to around 62% for the same reduction in the reactance seen from the wind park terminals. The results are presented in Fig. 18 and confirm the effectiveness of the proposed controller.

The LQR technique is proved to result in a robust controller and it is able to provide desired damping following small changes in the effective compensation level due to system impedance variations. However, the SSCI damping controller should be redesigned when the investments take place in the vicinity of the WP and cause a dramatic change in the transmission system (such as interconnecting the wind park to the system with another series compensated transmission line).

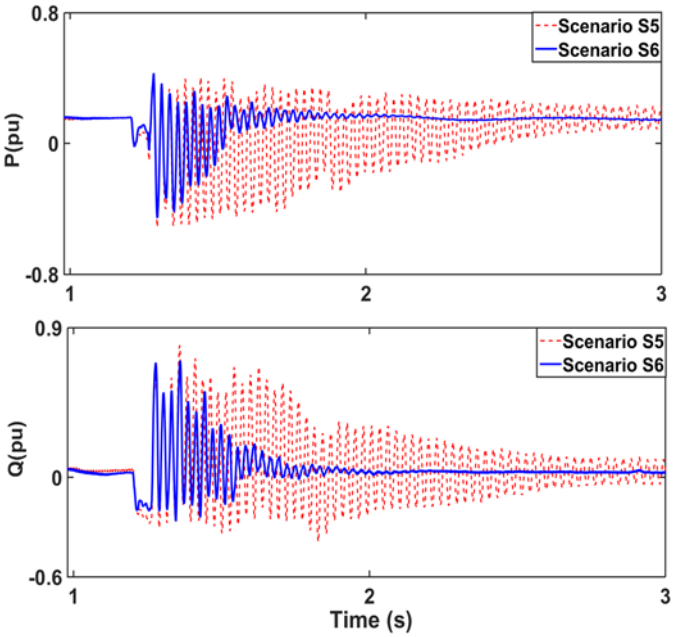

Fig. 13. Active and reactive powers in scenarios S5 and S6.

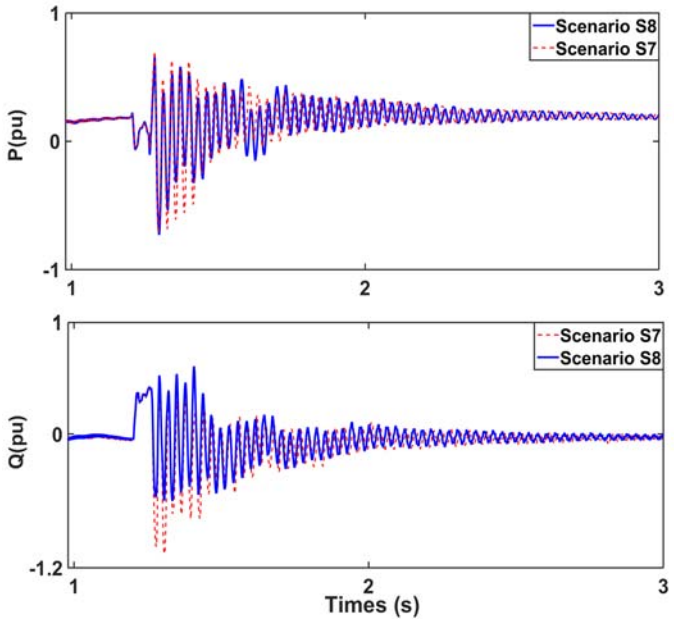

Fig. 14. Active and reactive powers in scenarios S7 and S8.

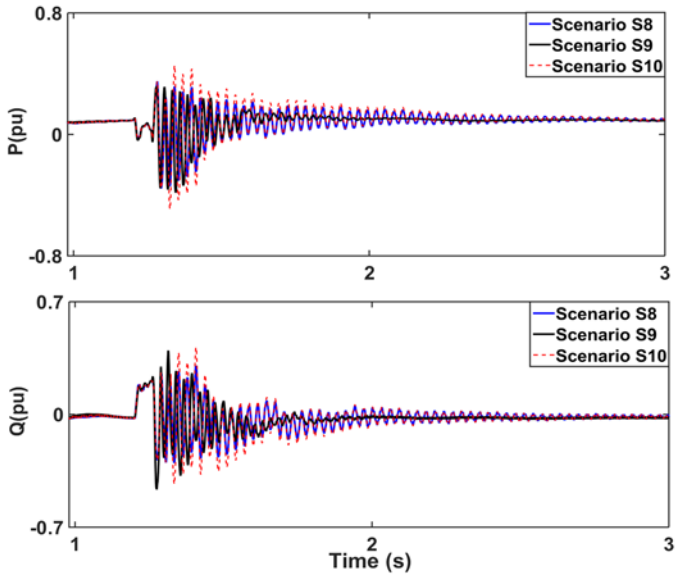

Fig. 15. Active and reactive powers in scenarios S8 - S10.

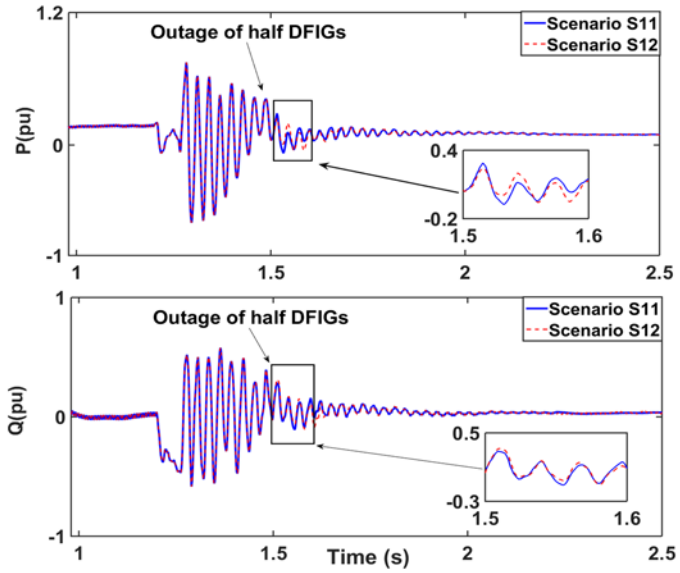

Fig. 16. Active and reactive powers in scenarios S11 - S12.

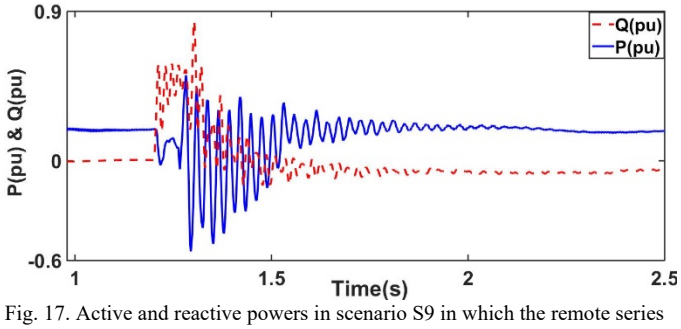

Fig. 17. Active and reactive powers in scenario S9 in which the remote series capacitor is bypassed following the fault.

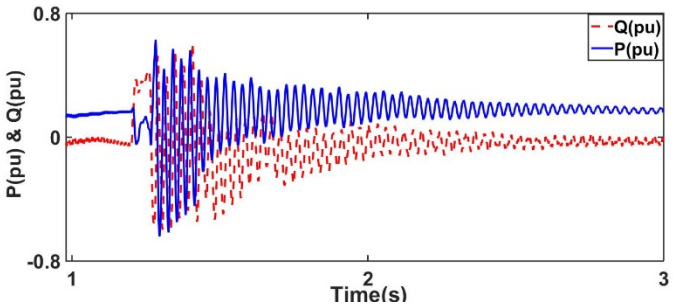

Fig. 18. Active and reactive powers in scenario S9 in which the System-1 equivalent impedance is reduced to 75%.

To confirm the accuracy of the aggregated model, simulation scenarios S1 and S2 are simulated using the aggregated representation of each cluster as shown in Fig. 19. Reader may refer to [30] for calculation of the aggregated WT model parameters, and to [33] for calculation of equivalent MV collector grid parameters.

The simulations with aggregated models are indicated with the "*" sign. It should be emphasized that, the aggregated models for the simulation scenarios S2 and S4 are identical (i.e. S2* and S4* are identical). As the waveforms are practically indistinguishable from the ones presented in Fig. 10, the differences are presented in Fig. 20 and Fig. 21.

As seen in Fig. 21, the results obtained with aggregated model are very close to the central SSCI controller implementation. The wind conditions and DFIG terminal voltages are slightly different at each WT. Hence, local SSCI damping controllers at the WTs produce slightly different output signals as well. However, the central SSCI damping controller uses the total active and reactive currents of the DFIG converters and this has an averaging effect. Moreover, each WTC receives the same signal produced by the central SSCI damping controller. As the WT in aggregated model assumes the average wind speed and same DFIG terminal voltage at each WT, it provides closer results to the central SSCI controller implementation scenario.

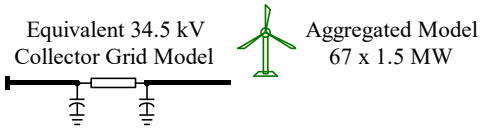

Fig. 19. Aggregated cluster model.

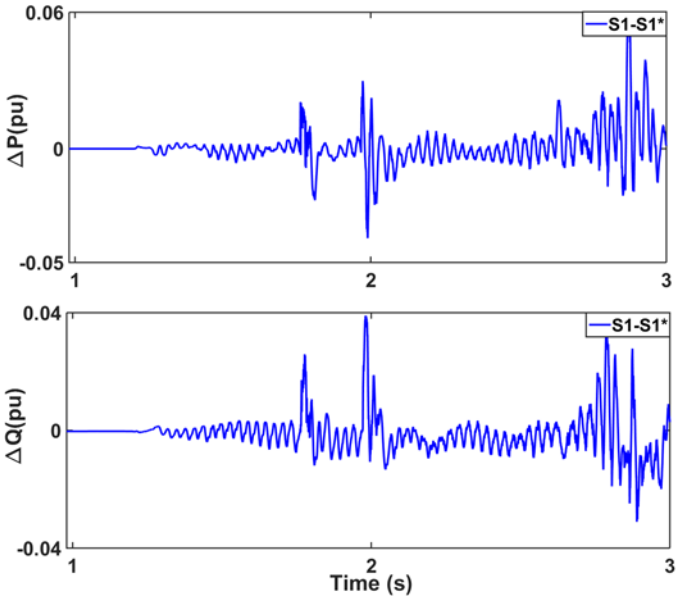

Fig. 20. Difference in active and reactive powers between S1 and S1*.

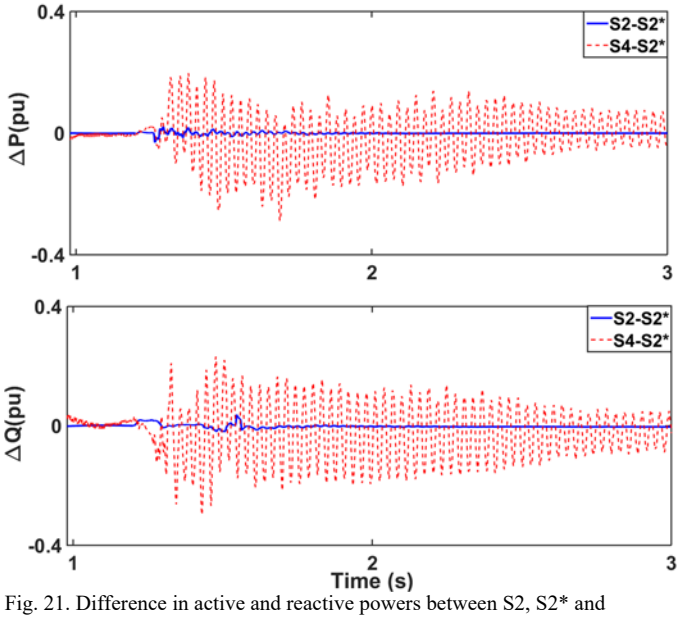

Fig. 21. Difference in active and reactive powers between S2, S2* and between S4, S2*.

VII. Conclusion

This paper contributes to the literature by proposing an effective implementation scheme for an LQR-based SSCI damping controller considering the WP realistic structure as well as the challenges due to communication requirements inside the WP. In the proposed implementation scheme, a local damping controller is integrated into the WTC for eliminating high rate data transfer requirement between the WTs and secondary control layer of the WP. The proper function is achieved by scaling the DFIG converter currents considering WT outages inside the WP. This information is available at WPC and it changes only when there is a change in the number of WTs in service (i.e. no continuous change). The performance is improved further by using an adaptive approach that modifies the damping controller considering number of units in service. The desired FRT operation of the DFIG is achieved by limiting the damping controller output signals dynamically to avoid saturating the DFIG converters.

To demonstrate the effectiveness of the proposed implementation scheme and compare its performance with the central implementation counterpart, EMT simulations are preformed using the complete WP model. The simulations demonstrated that

- Both implementations provided the desired performance (including the DFIG transient behavior). However, damping performance of the proposed local controller is slightly better compared to its central counterpart as it accounts for the different wind speed conditions and different reactive power generations at each WT.
- The proposed adaptive approach provides a significant increase in the damping controller performance for the WT outage scenarios.
- The proposed implementation does not only eliminate the high rate data transfer requirement between the WTs and secondary control layer of the WP, but also makes the system immune to the excessive (even unrealistic) communication delays. The central implementation counterpart is very vulnerable to communication delays and its usage may not be feasible in practice.
- The average wind speed assumption based aggregated model provides acceptable accuracy.

The LQR technique is proved to result in a robust controller and it is able to provide desired damping following small changes in the effective compensation level due to system impedance variations. However, the SSCI damping controller may need to be re-designed when the investments take place in the vicinity of the WP and cause a dramatic change in the transmission system (such as interconnecting the wind park to the system with another series compensated transmission line).

References

[1] L. Fan, C. Zhu, Z. Miao and M. Hu, "Modal Analysis of a DFIG-Based Wind Farm Interfaced With a Series Compensated Network," *IEEE Trans. Energy Convers.*, vol. 26, no. 4, pp. 1010-1020, Dec. 2011.

[2] L. C. Gross, "Sub-synchronous Grid Conditions: New Event, New Problem, and New Solutions," *37th Annual Western Protective Relay Conf.*, Spokane, WA, USA, Oct. 2010, pp. 1–19.

[3] G. D. Irwin, A. K. Jindal and A. L. Isaacs, "Sub-synchronous Control Interactions between Type 3 Wind Turbines and Series Compensated AC Transmission Systems," IEEE PES General Meeting, 2011.

[4] L. Wang, X. Xie, Q. Jiang, H. Liu, Y. Li and H. Liu, "Investigation of SSR in Practical DFIG-Based Wind Farms Connected to a Series-Compensated Power System," *IEEE Trans. Power Syst.*, vol. 30, no. 5, pp. 2772-2779, Sept. 2015.

[5] H. Liu, X. Xie, C. Zhang, Y. Li, H. Liu and Y. Hu, "Quantitative SSR Analysis of Series-Compensated DFIG-Based Wind Farms Using Aggregated RLC Circuit Model," *IEEE Trans. Power Syst.*, vol. 32, no. 1, pp. 474-483, Jan. 2017.

[6] V.B. Virulkar and G.V. Gotmare, "Sub-synchronous Resonance in Series Compensated Wind Farm: A review," *Renewable and Sustainable Energy Reviews*, Vol. 55, pp. 1010-1029, 2016.

[7] K. Narendra et al., "New microprocessor based relay to monitor and protect power systems against sub-harmonics," *IEEE Electrical Power and Energy Conference*, Winnipeg, MB, 2011, pp. 438-443

[8] J. Daniel *et al*., ERCOT CREZ Reactive Power Compensation Study, ABB Inc., Power Systems Division, Grid Systems Consulting, 2010, E3800-PR-00.

[9] U. Karaagac, S. O. Faried, J. Mahseredjian and A. A. Edris, "Coordinated Control of Wind Energy Conversion Systems for Mitigating Subsynchronous Interaction in DFIG-Based Wind Farms," *IEEE Trans. Smart Grid*, vol. 5, no. 5, pp. 2440-2449, Sept. 2014.

[10] D. H. R. Suriyaarachchi, U. D. Annakkage, C. Karawita, D. Kell, R. Mendis and R. Chopra, "Application of an SVC to damp sub-synchronous interaction between wind farms and series compensated transmission lines," *IEEE PES General Meeting*, San Diego, CA, 2012.

[11] H. Xie and M. M. de Oliveira, "Mitigation of SSR in presence of wind power and series compensation by SVC," *International Conference on Power System Technology*, Chengdu, 2014, pp. 2819-2826.

[12] S. Vivek and V. Selve, "SSR mitigation and damping power system oscillation in a series compensated wind generation system," *IEEE National Conference on Emerging Trends In New & Renewable Energy Sources And Energy Management*, Chennai, 2014, pp. 32-38.

[13] H. A. Mohammadpour and E. Santi, "Sub-synchronous resonance analysis in DFIG-based wind farms: Mitigation methods — TCSC, GCSC, and DFIG controllers — Part II," *IEEE Energy Conversion Congress and Exposition (ECCE)*, Pittsburgh, PA, 2014, pp. 1550-1557.

[14] H. A. Mohammadpour, Y. Shin and E. Santi, "SSR analysis of a DFIG-based wind farm interfaced with a gate-controlled series capacitor," *IEEE Applied Power Electronics Conference and Exposition - APEC 2014*, Fort Worth, TX, 2014, pp. 3110-3117.

[15] H. A. Mohammadpour, A. Ghaderi and E. Santi, "Analysis of sub-synchronous resonance in doubly-fed induction generator-based wind farms interfaced with gate - controlled series capacitor," *IET Generation, Transmission & Distribution*, vol. 8, no. 12, pp. 1998-2011, Dec. 2014.

[16] H.A. Mohammadpour and E. Santi, "Modeling and control of gate-controlled series capacitor interfaced with a DFIG-based wind farm," *IEEE Trans Ind Electron,* vol. 62, no. 2, pp. 1022-1033, Feb. 2015.

[17] M. Ghafouri, U. Karaagac, H. Karimi, S. Jensen, J. Mahseredjian and S. O. Faried, "An LQR Controller for Damping of Subsynchronous Interaction in DFIG-Based Wind Farms," *IEEE Trans. Power Syst.*, vol. 32, no. 6, pp. 4934-4942, Nov. 2017.

[18] H. A. Mohammadpour, A. Ghaderi, H. Mohammadpour, and E.Santi, "SSR Damping in Wind Farms Using Observed-State Feedback Control of DFIG Converters," *Electric Power Systems Research*, Volume 123, 2015, Pages 57-66.

[19] H. A. Mohammadpour and E. Santi, "Optimal Adaptive Sub-synchronous Resonance Damping Controller for a Series-Compensated Doubly-Fed Induction Generator-based Wind Farm," *IET Renewable Power Generation*, vol. 9, no. 6, pp. 669-681, 8 2015.

[20] M. A. Chowdhury, M. A. Mahmud, W. Shen and H. R. Pota, "Nonlinear Controller Design for Series-Compensated DFIG-Based Wind Farms to Mitigate Subsynchronous Control Interaction," *IEEE Trans. Energy Convers.*, vol. 32, no. 2, pp. 707-719, June 2017.

[21] J. Taherahmadi, M. Jafarian and M. N. Asefi, "Using Adaptive Control in DFIG-based Wind Turbines to Improve the Subsynchronous Oscillations of nearby Synchronous Generators," *IET Renewable Power Generation*, vol. 11, no. 2, pp. 362-369, 2 8 2017.

[22] P. H. Huang, M. S. El Moursi, W. Xiao and J. L. Kirtley, "Subsynchronous Resonance Mitigation for Series-Compensated DFIG-Based Wind Farm by Using Two-Degree-of-Freedom Control Strategy," *IEEE Trans. Power Syst.*, vol. 30, no. 3, pp. 1442-1454, May 2015.

[23] C. Zhu, L. Fan and M. Hu, "Control and Analysis of DFIG-based Wind Turbines in a Series Compensated Network for SSR Damping," *IEEE PES General Meeting*, Minneapolis, MN, 2010, pp. 1-6.

[24] U. Karaagac, H. Saad, J. Peralta, J. Mahseredjian, "Doubly-fed Induction Generator based Wind Park Models in EMTP-RV," April 2015, Polytechnique Montréal, research report.

[25] "Grid Code - High and Extra High Voltage," E.ON Netz GmbH, Bayreuth, Germany, April 2006.

[26] J. M. Garcia, "Voltage Control in Wind Power Plants with Doubly Fed Generators," Ph.D. dissertation, Aalborg Univ., Denmark, Sep. 2010.

[27] S. Skogestadand I. Postlethwaite, "Multivariable Feedback Control, Analysis and Design," Wiley, Nov 4, 2005.

[28] G. R. Duan and H. H. Yu, LMIs in Control Systems: Analysis, Design and Applications, Boca Raton, FL, USA: CRC Press, Jun. 2013.

[29] J. Mahseredjian, S. Dennetière, L. Dubé, B. Khodabakhchian and L. Gérin-Lajoie: "On a New Approach for the Simulation of Transients in Power Systems," *Electric Power Systems Research*, Volume 77, Issue 11, September 2007, pp. 1514-1520.

[30] U. Karaagac, J. Mahseredjian, S. Jensen, R. Gagnon, M. Fecteau and I. Kocar, "Safe Operation of DFIG based Wind Parks in Series Compensated Systems," Early access article, *IEEE Trans. Power Del.,* DOI: 10.1109/TPWRD.2017.2689792.

[31] B. Badrzadeh, M. Sahni, D. Muthumuni, Y. Zhou and A. Gole, "Sub-Synchronous Interaction in Wind Power Plants – Part I: Study Tools and Techniques," in *Proc IEEE PES Gen. Meet.*, San Diego, CA, July 22-26, 2012.

[32] B. Badrzadeh, M. Sahni, Y. Zhou, D. Muthumuni, and A. Gole, "General Methodology for Analysis of Sub-Synchronous Interaction in Wind Power Plants," *IEEE Trans. On Power Systems*, 2013, vol. 28, no.2, pp. 1858-1869.

[33] E. Muljadi, C.P. Butterfield, A Ellis, J. Mechenbier, J. Hochheimer, R. Young, N. Miller, R. Delmerico, R. Zavadil, and J.C. Smith, "Equivalencing the Collector System of a Large Wind Power Plant," IEEE PES General Meeting, 2006.